Journal of Photochemistry & Photobiology, A: Chemistry 433 (2022) 114176

Contents lists available at ScienceDirect

Journal of Photochemistry & Photobiology, A: Chemistry

journal homepage: www.elsevier.com/locate/jphotochem

Photocatalytic transformation of Rhodamine B to Rhodamine-110 – The mechanism revisited

Anna Jakimińska, Miłosz Pawlicki, Wojciech Macyk *

Faculty of Chemistry, Jagiellonian University, ul. Gronostajowa 2, 30-387 Kraków, Poland

ARTICLE INFO

Keywords:
Rhodamine B
Rhodamine 110
TiO_2
Photodegradation
N-deethylation

ABSTRACT

Understanding of the TiO_2-assisted phototransformations observed for fundamentally important derivatives of Rhodamine B is expected to bring consistent and eventually comprehensive knowledge on behavior of this dye. The photocatalytic transformations of Rhodamine B in solution irradiated with visible light embrace an *N*-deethylation process eventually forming Rhodamine-110 rather than degradation of the chromophore. The *N*-deethylation of Rhodamine B was studied in solution and for the first time in the solid state. In this work, the influence of the wavelength of incident light on the photocatalytic processes involving Rhodamine dyes, is presented. The results indicate that the selection of wavelength is crucial to govern the pathway of RhB degradation. The *N*-deethylation process does not require reactive oxygen species, as assumed in literature, but the photoinduced electron transfer between the adsorbed RhB molecule and the TiO_2 support, followed by radical transformations of the dye, plays a key role.

1. Introduction

Rhodamine B (RhB) is one of the most explored dyes in photocatalysis [1–3] and among methylene blue and methyl orange its degradation enables estimation of the photocatalytic activity of various materials [2]. Although all these dyes are not fully photostable, they are vividly coloured which facilitates the observation of their transformation progress by UV–vis spectroscopy. Nevertheless, organic dyes are mostly large and complex compounds with their own photochemistry, and the degradation pathways during photocatalytic processes are very often oversimplified. Moreover, organic dyes, due to their strong absorption of visible light can sensitize the semiconductors which can make photocatalytic degradation more facile. The transformation routes are often complicated, but for Rhodamine B some authors made great efforts to resolve them [3–5].

Rhodamine B (**1**, Scheme 1) is a cationic xanthene dye with a bright pink color exhibiting a strong orange fluorescence centered at λ_{max} = 586 nm caused by the forced delocalization involving the flanking amine groups that introduces a positive charge. Its absorption spectrum has the maximum at 554 nm for the zwitterion form (**1′**) – the most common variant of the dye, stable in a broad range of pH with the negative charge on the carboxyl group and the positive one on the xanthene chromophore. The conjugation observed within the chromophore can be described by three resonance forms (**1′**, **1′′** and **1′′′**) delocalizing the positive charge between nitrogen atoms (**1′** and **1′′′**) and *ipso*-carbon atom with the benzoic acid moiety attached (**1′′**) what allows the dye to form a non-fluorescent, neutral and colorless spirolactone **2**, Scheme 1). Rhodamine B under irradiation with visible light in the presence of the photocatalyst undergoes the *N*-deethylation process which involves a subsequent detachment of ethyl groups from the amino nitrogen atoms, resulting in a hypsochromic shift of absorption and emission maxima. The final product of the *N*-deethylation is greenish Rhodamine-110 (**3**, Rh-110, Scheme 1) exhibiting an intense and bright green fluorescence. The process takes place when the photocatalyst is sensitized by RhB excited with visible light. Otherwise, when the photocatalyst is directly excited, RhB undergoes non-selective oxidation by generated reactive oxygen species, resulting in the chromophore decomposition.

There are certain factors including the spectral range of light [3,6], and ζ potential of the catalyst correlated, inter alia, with pH of the solution influencing the *N*-deethylation process [5,7]. The most efficient approach for observing the *N*-deethylation consists of the dye adsorption at the photocatalyst through positively charged amino groups what leads to a necessity of a negative charge presence on the photocatalyst surface requiring the ζ potential to be negative. The ζ potential depends also on the photocatalyst nature but sometimes it can be adjusted by changing pH of the solution without strong influence on the zwitterion

* Corresponding author.
E-mail address: macyk@chemia.uj.edu.pl (W. Macyk).

https://doi.org/10.1016/j.jphotochem.2022.114176
Received 3 May 2022; Received in revised form 18 July 2022; Accepted 25 July 2022
Available online 28 July 2022

form of RhB reported as a stable dye in the wide pH range (from 3 to 12) [8]. Nevertheless, the effect remains the same and after adsorption of RhB at the photocatalyst surface via amino groups the *N*-deethylation process occurs under visible light irradiation.

The *N*-deethylation process eventually agreed by most authors to be stepwise has been widely examined with GC–MS, UV–vis spectroscopy or HPLC [4,5,9]. Merka et al. and Chen et al. stated that the adsorption is crucial, and it is the main factor that affects the efficiency of the transformation of RhB into Rh-110. Both groups and other authors suggest also that reactive oxygen species are responsible for the detachment of ethyl groups [4,5,10]. Liang et al. stated also that the superoxide radicals take part in creation of the transient form which protects the xanthene chromophore and subsequently enables the *N*-deethylation via hydroxyl radicals [3]. However, results obtained by different groups vary mostly in the range of the light – some of them even report that the *N*-deethylation process can be driven under UV radiation [11]. Therefore, there is a need to evaluate the dependence of this process on incident light. These discrepancies indicate that the real mechanism of *N*-deethylation still remains unclear.

This work focuses on the examination of the dependence of the *N*-deethylation process on the wavelength of incident light and reaction conditions. Moreover, for the first time the *N*-deethylation process taking place in the solid state is reported. A thorough analysis revealed the new features emerging in the TiO_2/RhB system. Therefore, basing on the results, the new light was shed on the mechanism of Rhodamine B transformations under visible light irradiation.

2. Experimental

2.1. Reagents

Titanium(IV) isopropoxide (TTIP) (Sigma-Aldrich, >97 %), ethanol (Avantor POCh, for analysis, >99.8 %), ethylene glycol (EG) (Avantor POCh, for analysis, >99 %), Pluronic P-123 (Aldrich, M ≈ 5800), Rhodamine B (RhB) (Warchem, pure, 95 %), HCl (Chempur, pure for analysis, 35–38 %), LUDOX (Sigma-Aldrich), isopropyl alcohol (IPA) (Pure-Land, pure for analysis), ethylenediaminetetraacetic acid disodium salt (EDTA) (Chempur, pure for analysis), potassium persulfate ($K_2S_2O_8$) (Loba-Chemie, pure), KNO_3 (Sigma-Aldrich, pure) and methanol (Avantor, HPLC grade) were used without further purification. Deionized water was obtained using Hydrolab deionizer HLP 10UV (0.05 μS, t = 20 °C).

2.2. Synthesis

The TiO_2 material was synthesized via solvothermal method according to the protocol similar to that reported by Zhang et al. [12] and is described in SI.

2.3. Characterization

The SEM analysis was performed using Tescan Vega 3 microscope with LaB_6 cathode (30 kV). The microscope was equipped with the EDS detector (Oxford Instruments, X-act, SDD 10 mm^2). Silicon wafers were used as substrates for imaging to provide an ideally flat surface. X-ray diffractograms (XRD) were recorded using Rigaku MiniFlex 600 diffractometer equipped with the Cu lamp (K_α radiation wavelength – 1.5406 Å) with the Ni K_β filter. The scan step was 2° (2θ) and the scan speed was 10°/min.

Zeta potential of TiO_2 in the aqueous suspension was determined using a Malvern Panalytical Zetasizer Nano ZS instrument.

Photoelectrochemical measurements were carried out using the photoelectric spectrometer equipped with the 150 W xenon lamp (Instytut Fotonowy). The three-electrode cell was used with Ag/AgCl (in 3 mol/dm^3 KCl) electrode, Pt wire and ITO foil (Sigma-Aldrich, 60 Ω/sq) covered with a thin film of the examined material, set as a reference, counter and working electrodes, respectively. 0.1 mol/dm^3 KNO_3 solution in water was used as the electrolyte and argon was purged through the cell during the whole experiment. The applied potential was changed from –200 to 800 mV with the 100 mV step.

2.4. Photoactivity tests

Tests with 10^{-5} mol/dm^3 RhB aqueous solution were performed to estimate photoactivity of the system. LED diodes (Instytut Fotonowy) with different λ_{max} of emitted light – 405 nm with the 400 nm cut-off filter (described further as 405 nm), 465 nm and 520 nm were used as the light sources. Tests were carried out both in solution and in the solid state. Typically, 10.5 ml of RhB solution and 3.5 ml of the suspension of TiO_2 (4 g/l) in deionized water were mixed and poured into a quartz cuvette. Irradiation of suspensions took 5 h. The samples were taken every hour and were centrifuged. Absorbance of the supernatant was

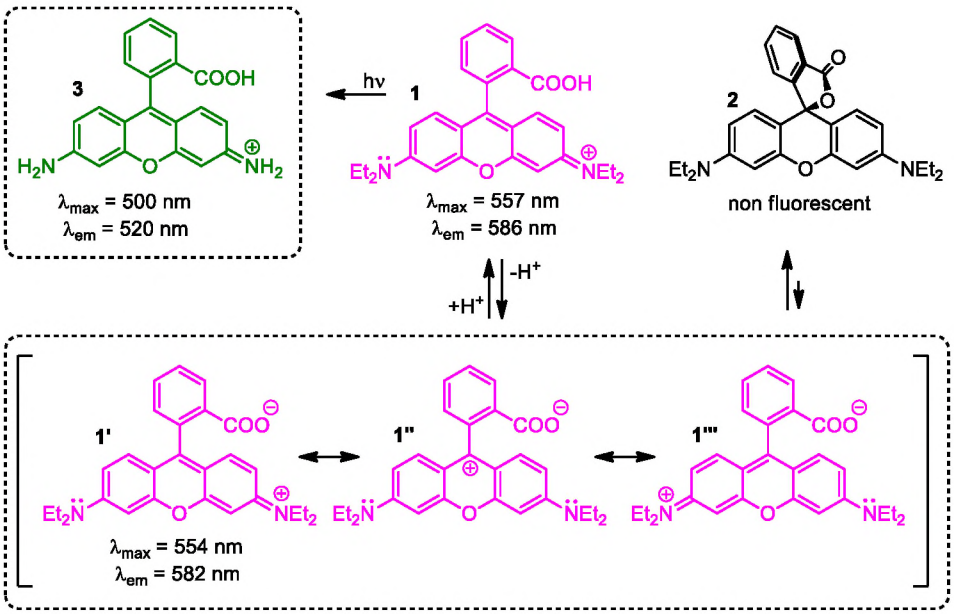

Scheme 1. Transformations of Rhodamine B.

measured using HP 8453 Diode Array spectrophotometer. The same procedure was applied to perform the tests with scavengers (described in SI), except of adding 10 μl of isopropyl alcohol, 140 μl of EDTA solution (0.1 mol/dm^3) or 140 μl of potassium persulfate solution (0.1 mol/dm^3), as mentioned in the description of the appropriate experiment. To establish the influence of oxygen on the photocatalytic processes, argon or oxygen was purged through the suspension for at least 10 min and afterwards the cuvette was sealed.

Tests in the solid state were performed for 6 h and the fluorescence emission spectra were measured every hour using the Fluorolog-3 (Horiba Jobin-Yvon) spectrofluorometer equipped with the 450 W Xe lamp. For these tests, 100 μl of RhB solution (10^{-5} mol/dm^3) was cast on the TiO_2 thin film on a glass substrate and subsequently evaporated, then fluorescence of the sample was measured ($\lambda_{exc} = 500$ nm). To avoid misinterpretations, samples were not removed from the holder during irradiation to ensure that the spectra were always recorded for the same area.

Photocurrent measurements were carried out with the setup from Instytut Fotonowy described in section 2.3. The three-electrode system consisted of Ag/AgCl (in 3 mol/dm^3 KCl) electrode, Pt wire and ITO foil. The KNO_3 solution (0.1 mol/dm^3) in water was used as the electrolyte and was deaerated with argon flow during measurements. The working electrode was prepared by casting the TiO_2 layer on the ITO foil, then the electrode was dried and subjected to the measurements. Subsequently, to record the changes after RhB adsorption, the prepared electrode was immersed in RhB aqueous solution (10^{-5} mol/dm^3) and after drying, the measurements were performed again to ensure that the changes originated only from the modification with RhB. Moreover, the same experiments for TiO_2 and TiO_2/RhB were performed with an addition of methanol (1 % vol.) to distinguish whether the RhB influence (especially in the range of 400–500 nm) is not only the aftermath of its oxidation causing possibly the so-called photocurrent doubling effect.

Additional data, along with description of other experimental procedures and results, are provided in the Supporting Information.

3. Results and discussion

3.1. Characterization of TiO_2

To establish the properties of the synthesized photocatalyst, its full characterization was performed with application of SEM, EDS and XRD techniques. The SEM measurements revealed the flake-like morphology (Fig. 1a), while EDS analysis confirmed the material composition. The XRD analysis unveiled the presence of both anatase and rutile phases in the material, and the shape of the peaks indicates that TiO_2 is composed of very small crystallites (Fig. 1b).

The diffuse reflectance spectrum of the obtained TiO_2 was recorded and subsequently transformed using the Kubelka-Munk function and the Tauc function for indirect band-gap semiconductors, $(\alpha h\nu)^{1/2}$ (Fig. S1). The absorption edge, estimated from the Kubelka-Munk spectrum, lies around 350 nm, so the material absorbs ultraviolet light only. The band gap energy estimated from the Tauc plot equals to 3.5 eV. It is relatively high and confirms that the photocatalyst should be active only under UV irradiation.

To assess adsorption capability, ζ potential measurements were carried out in deionized water, to provide conditions similar to those in the photocatalyst suspension used in the RhB degradation tests. The measurements revealed the potential equal to –41.6 mV, indicating a good stability of the TiO_2 colloid. A negatively charged surface of the photocatalyst is especially advantageous for adsorption of cationic dyes, such as RhB. Adsorption of RhB via positively charged amino groups facilitates the *N*-deethylation process [4]. For comparison, under similar pH conditions the reference P-25 material exhibits a positive ζ potential equal to 26.5 mV. This significant difference between P-25 and the synthesized material strongly influences adsorption of RhB and therefore the pathway of its photocatalytic transformations.

To estimate the photoactivity of the material photoelectrochemical measurements were conducted. Transient photocurrent response measurements for bare TiO_2 material confirmed the photoactivity in the ultraviolet range with the highest IPCE around 330 nm. The activity decreases with increasing wavelength to disappear at around 400 nm. The switch from cathodic to anodic photocurrents is noticeable when changing from negative to positive potentials. The map shown in Fig. 2 depicts the dependence of IPCE on the incident light wavelength and the applied potential. IPCE values are not very high, pointing at a low

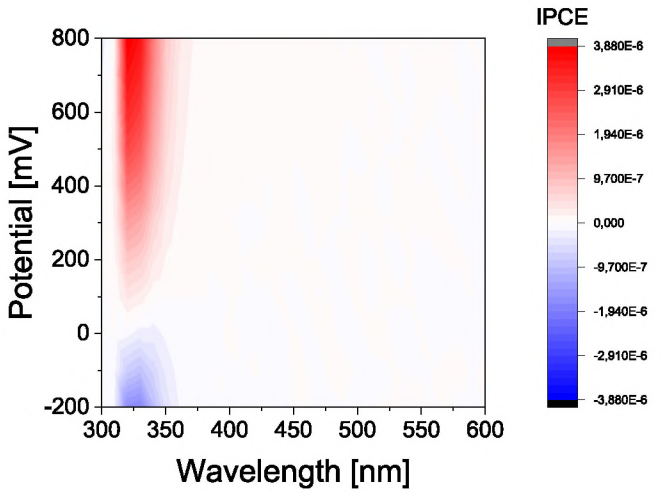

Fig. 2. IPCE dependence on the incident light wavelength and applied potential.

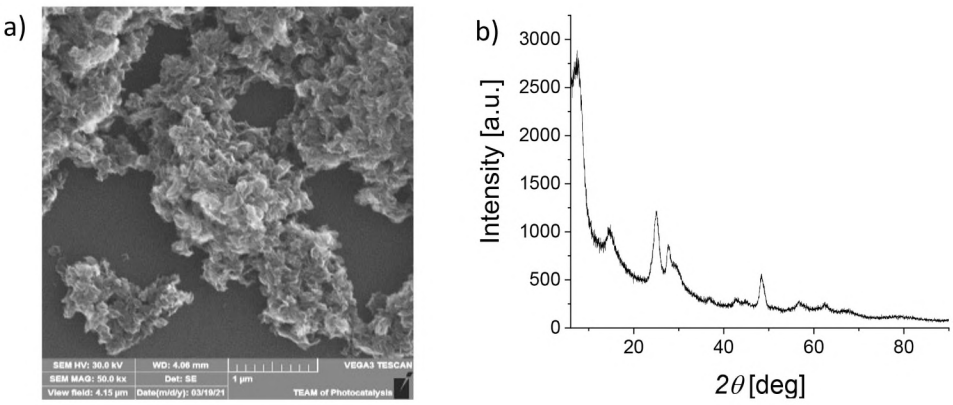

Fig. 1. SEM image (a) and XRD pattern (b) of the TiO_2 material.

efficiency of the charge carriers separation. Performed experiments confirmed that the studied TiO_2 material is scarcely active in the visible light range ($\lambda > 400$ nm).

3.2. Photocatalytic transformation of RhB

The photocatalyst suspension in RhB aqueous solution was irradiated for 5 h with different LEDs. In all cases hypsochromic shift of the main absorption maximum was observed indicating appearance of Rhodamine 110 (Rh-110) in the system. Rh-110 is the product of full *N*-deethylation of RhB and it emerges during indirect photocatalytic degradation of RhB on some photocatalysts. For the best conversion, the RhB adsorption on the photocatalyst surface via amino groups is advantageous. Such adsorption mode is preferential at negatively charged surface of the studied TiO_2 material (see section 3.1.), resulting in a proximity of RhB xanthene chromophores to the photocatalyst surface.

During irradiation with three different LEDs: 405, 465 and 520 nm, it turned out that the RhB to Rh-110 conversion is wavelength dependent. The absorption spectra of these dyes, as well as emission spectra of the LEDs, are presented in Fig. 3. RhB and Rh-110 absorb poorly around 405 nm, but strongly at 465 nm (Rh-110) and 520 nm (RhB), so the dyes can be excited efficiently by the corresponding diodes, what reflects in different progress of photoinduced transformations. For the LED 405 nm almost full RhB to Rh-110 conversion is observed, whereas for longer wavelengths, 465 and 520 nm, degradation of both RhB and generated Rh-110 prevails (Fig. 4a). To confirm, that *N*-deethylation process requires the photocatalyst, tests of RhB photostability under the same conditions as for photocatalytic tests, but in the absence TiO_2, were performed (Fig. 4b). It turned out that without photocatalyst the decrease in absorbance is much less significant, and no formation of the band characteristic for Rh-110 is observed during irradiation. Moreover, in the presence of TiO_2 the *N*-deethylation process takes place only during irradiation with visible light [6], suggesting that the excited state of RhB is involved in this process. Taking into account the lack of the TiO_2 activity induced by visible light, these results denote that RhB decolorization and *N*-deethylation processes are the effects of TiO_2-catalyzed photodegradation of the dyes. This process can involve, in analogy to the photosensitization, the electron transfer from the excited dye molecule to the conduction band of TiO_2. The injected electrons can further take part in reduction reactions, including generation of reactive oxygen species (ROS). This explains the higher rates of the dyes degradation upon irradiation with the LEDs emitting light efficiently absorbed by the dyes.

To reveal the influence of oxygen on the degradation of rhodamines, the tests with increased and decreased oxygen concentration were performed. To decrease oxygen concentration, argon was purged through the suspensions for 10 min and then the sealed cuvettes were irradiated with 405, 465 or 520 nm LEDs. Decrease in oxygen concentration

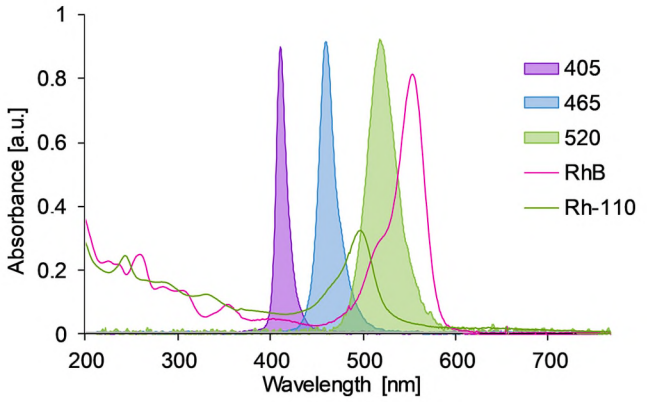

Fig. 3. Absorption spectra of RhB and Rh-110 with emission spectra of used LEDs (405, 465, 520 nm).

slowed down the degradation process and favored the RhB to Rh-110 conversion (Fig. 4c). Nevertheless, the wavelength dependence is still clear and follows the same manner as for non-deaerated suspensions. Moreover, for the test involving irradiation at 405 nm in Ar-saturated suspension, after the first hour a significant decrease in absorbance without any hypsochromic shift of the maximum can be observed. After this time, the absorbance rises again, and the process follows the *N*-deethylation path. The decrease of absorbance may indicate formation of the leuco form of RhB, which is the product of a direct reduction of RhB with electrons [13]. These results emphasize the role of oxygen in the system – in oxygen-containing system O_2 can act as the electron scavenger leading to the formation of $O_2^{\bullet-}$ and preventing generation of the leuco form.

On the contrary, when the oxygen was purged for 10 min through the system to increase its concentration, the fastest rhodamines removal was observed for 465 and 520 nm LEDs (Fig. 4d). For the 405 nm LED almost no difference between the tests with and without increased oxygen concentration could be noticed. It shows that the production of ROS via photoinduced electron transfer to TiO_2 from the dyes is most efficient when they are excited within their absorption bands. Therefore, when neither rhodamines nor TiO_2 absorb effectively (405 nm), the amount of oxygen in the system influences the process negligibly, indicating, that the reactive oxygen species cannot reach higher concentrations.

All these tests lead to another conclusion – the RhB to Rh-110 conversion is most efficient at low concentration of reactive oxygen species. To evaluate whether ROS can be produced in the TiO_2/RhB system, or RhB undergoes a direct reaction with surface trapped charge carriers, the solutions of $K_2S_2O_8$, EDTA or pure isopropyl alcohol (IPA) were added as the electron, hole and hydroxyl radical scavengers, respectively. The results of these tests are described in Supporting Information and presented in Fig. S2.

3.3. Solid state experiments

The RhB solution was cast onto glass substrates covered with TiO_2 thin film and dried. Subsequently, the samples were irradiated with the same LEDs as in the above-described tests. The irradiation lasted 6 h and every hour emission spectrum was recorded (Fig. 5).

For the samples irradiated at 465 and 520 nm the decrease in the fluorescence intensity and slight hypsochromic shifts of emission maximum were observed. For the 405 nm irradiation, the decrease is associated with the strongest hypsochromic shift. The irradiated part of the initially pink sample turned greenish, indicating the generation of *N*-deethylation products. The new maximum is not completely separated which may point out the contribution of not fully deethylated Rhodamine species.

Upon irradiation at 520 nm degradation prevails over transformation. The trace of a new maximum around 530 nm appears, but the maximum does not separate and both maxima vanish with time simultaneously. Similarly, under 465 nm irradiation the degradation process also prevails, and the new maximum can be hardly recognized, but still a slight hypsochromic shift of the RhB emission maximum is observed. These observations support the hypothesis that in this range of radiation (465 nm) the *N*-deethylation product sensitizes the photocatalyst and undergoes self-degradation [14].

3.4. Fluorescence lifetime measurements

To prove the concept of an efficient sensitization of the photocatalyst by Rhodamines excited with appropriate wavelengths, the fluorescence lifetime measurements were conducted. Lifetimes were measured under irradiation with 560 and 460 nm pulse LEDs and fluorescence decays were recorded for bare RhB solution and the solution with TiO_2 suspension. The experiment was also performed for the *N*-deethylation product obtained after 5 h of RhB solution irradiation with 405 nm LED.

The decay curves of RhB recorded under excitation with 560 nm LED

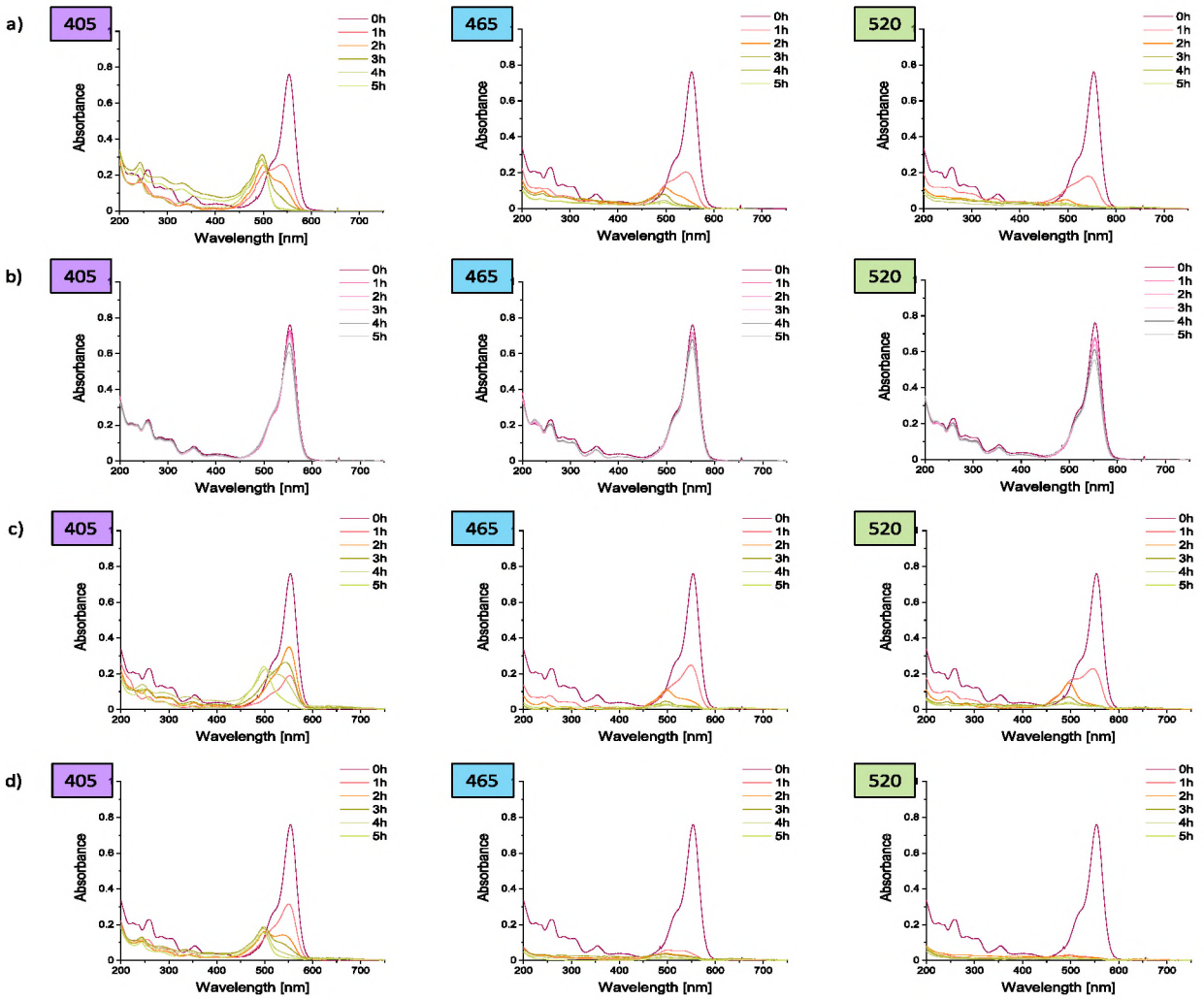

Fig. 4. Changes in absorption spectra of RhB recorded during irradiation with different LEDs in the system with TiO_2 (a), without the photocatalyst (b), with TiO_2 purged with Ar (c) and with TiO_2 purged with O_2 (d).

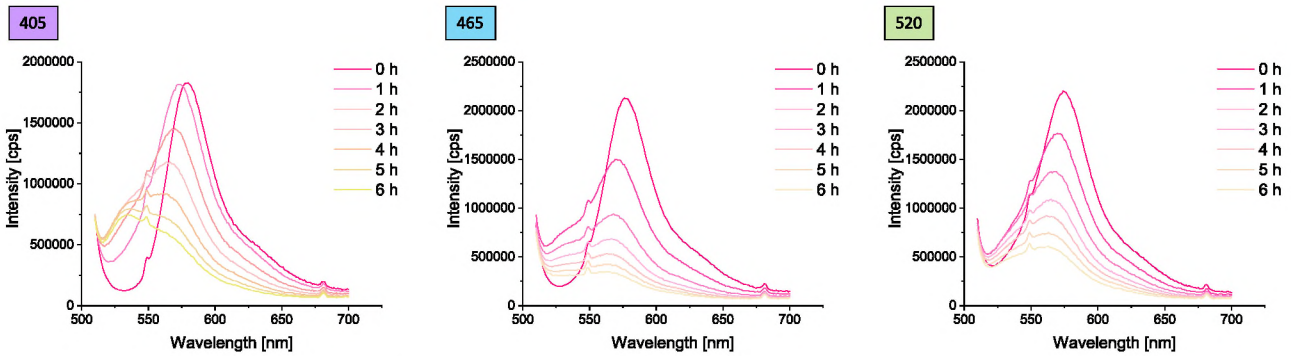

Fig. 5. Changes in the emission spectra of RhB on TiO_2 during irradiation with different LEDs in solid state. Excitation wavelength – 500 nm.

indicate the evident change in the decay from monoexponential to biexponential one, which suggests occurrence of the relaxation processes different from the light emission. These processes can be attributed to the sensitization of TiO_2 by excited RhB molecules. However, under excitation with 460 nm LED, this phenomenon is not noticeable. Corresponding decay curves and tables summarizing measured lifetimes are presented in Fig. S3. These results lead to the conclusion that the sensitization efficiency depends on the excitation wavelength, as RhB absorbs very well around 560 nm but relatively weakly around 460 nm.

Moreover, the decay curves for the *N*-deethylation product show that under 460 nm irradiation the fluorescence lifetime is shorter in the presence of TiO_2 than for the bare solution, and the curve follows a biexponential decay. On the contrary, for 560 nm irradiation, only the component from the scattered light can be observed on the decay curve in the system containing TiO_2 (Fig. S4). The decay recorded for the solution of *N*-deethylation product under irradiation at 560 nm in the

absence of TiO_2 can be derived from the fraction of not fully *N*-deethylated products.

On the basis of these results, it can be stated that the wavelength of the incident light strongly affects the pathways of Rhodamine B transformation. Due to the different spectral ranges of absorption of the parent dye and the product, which both can sensitize TiO_2 and cause the production of reactive oxygen species, the enhancement of degradation can be observed when the system is irradiated at suitable wavelengths. This explains well the results observed during photocatalytic tests. Under irradiation at 520 nm, degradation is the fastest, because the concentration of RhB which sensitizes the semiconductor is the highest. At 465 nm, where the *N*-deethylation product can sensitize TiO_2, degradation is somewhat slower. This is due to the lower absorption of RhB at this wavelength which results in a lower efficiency of ROS generation. When Rh-110 concentration increases the overall degradation process accelerates. Differences between solid state tests and tests in suspensions result from a limited diffusion in the solid state. Therefore, for dry samples (in contrary to the suspensions), under irradiation at 465 nm the *N*-deethylation product can be hardly observed, while at 520 nm both dyes degrade, however, the maximum of *N*-deethylation product is better evolved in this case.

The most intriguing is the case when 405 nm LED is involved. Both in the suspension and solid state, the RhB to Rh-110 transformation prevails. The dyes absorb negligibly in this range, so the sensitization leading to the ROS generation is ineffective, in agreement with the tests involving a higher concentration of oxygen in the system.

3.5. Mechanism

A key to elucidate the mechanism of RhB transformations is the analysis of activity of the system, both photochemical and photoelectrochemical [14,15]. IPCE measurements (Fig. 6, S5, S6) reveal photosensitization of TiO_2 by RhB at the spectral range of the main absorption band of the dye, particularly pronounced in the cathodic photocurrents range (blue area in Fig. 6 and S5). Moreover, anodic photocurrents (red area) are amplified within 400–450 nm, which corresponds to a weak absorption of RhB. Such behaviour is also evident after addition of methanol to the system, indicating that the effect results from RhB presence and is not the photocurrent doubling effect caused by oxidation of RhB or its intermediates (Fig. S5, S6). The excitation at this range results in a very selective transformation of RhB to Rh-110, as evidenced by the isosbestic point observed in Fig. 4a. The *N*-deethylation process is initiated by the electron transfer from the excited dye molecule to the conduction band of TiO_2 (Scheme 2). In this way the dye molecule is oxidized to a radical cation, $RhB^{\bullet+}$, with the unpaired electron localized at the nitrogen atom $\mathbf{1}^{\bullet+}$. This intermediate can isomerize to spiroradical $\mathbf{2}^{\bullet+}$, that based on the DFT calculations, is more stable by 16 kcal/mol, suggesting a significant contribution of this form in the *N*-deethylation process. The spiroform **2** (Scheme 1) is more stable by ~ 7 kcal/mol than the zwitterionic derivative **1′** based on the DFT calculations performed at the same level of theory as for the $\mathbf{1}^{\bullet+}/\mathbf{2}^{\bullet+}$ couple. The DFT optimized spin distribution (Fig. S7) has shown an expected symmetry and stability for $\mathbf{2}^{\bullet+}$, not observed for $\mathbf{1}^{\bullet+}$.

The formation of radical cation $\mathbf{1}^{\bullet+}/\mathbf{2}^{\bullet+}$ is followed by a radical deethylation of $-N(Et)_2$ group, which in the presence of water leads to formation of ethanol and –N(Et)H, as well as formation of deethylated spiroradical $\mathbf{2}^{\bullet+}$ expected to show lower energy than deethylated $\mathbf{1}^{\bullet+}$. Further excitation of the dye leads to a stepwise removal of the remaining ethyl groups. In this way a completely deethylated product (Rh-110) is formed. It is worth noting, that in contrast to numerous reports [3,4,5,9,10] this mechanism does not require ROS. This conclusion is supported by the fact, that RhB to Rh-110 transformation needs the presence of TiO_2, but is most efficient under conditions when reactive oxygen species are not generated efficiently (neither TiO_2 nor RhB should be excited within their main absorption bands). As shown in Fig. 4a, c, and d for 405 nm irradiation, the presence of oxygen does not lead to the degradation of the dye, but facilitates a quantitative transformation of RhB to Rh-110, pointing at the important role of O_2 as the electron scavenger preventing the RhB transformation to the leuco form. Concluding, ROS, including $HO^{\bullet}$, are involved in a complete degradation of the dyes rather than in the *N*-deethylation process.

4. Conclusions

In this work the influence of irradiation conditions, oxygen concentration and scavengers on the Rhodamine B *N*-deethylation process was analyzed. The tests with scavengers indicated that neither hydroxyl radicals nor holes are responsible for *N*-deethylation. It turned out, that the *N*-deethylation process competes with non-selective oxidation reactions. The relative efficiencies of these processes depend strongly on the incident light wavelength. The *N*-deethylation product, Rhodamine-110, predominates upon irradiation at 405 nm, i.e. light poorly absorbed by any component of the system (RhB, Rh-110 and TiO_2). Under such conditions, hydroxyl radicals are not generated efficiently, while RhB is oxidized to $RhB^{\bullet+}$, which subsequently undergoes a spontaneous *N*-deethylation. However, irradiation with light efficiently absorbed by the dyes facilitates their degradation process due to the ROS formation through the sensitization of TiO_2 by the excited dyes.

The RhB phototransformations are summarized in Scheme 3. Until now, the most commonly referred mechanism encompasses a selective *N*-deethylation through cleavage of N—C bonds with ROS (Scheme 3a), although $HO^{\bullet}$ may attack several fragments of the RhB molecule. We have demonstrated, that the *N*-deethylation process itself is not governed by reactive oxygen species, but by the photoinduced electron

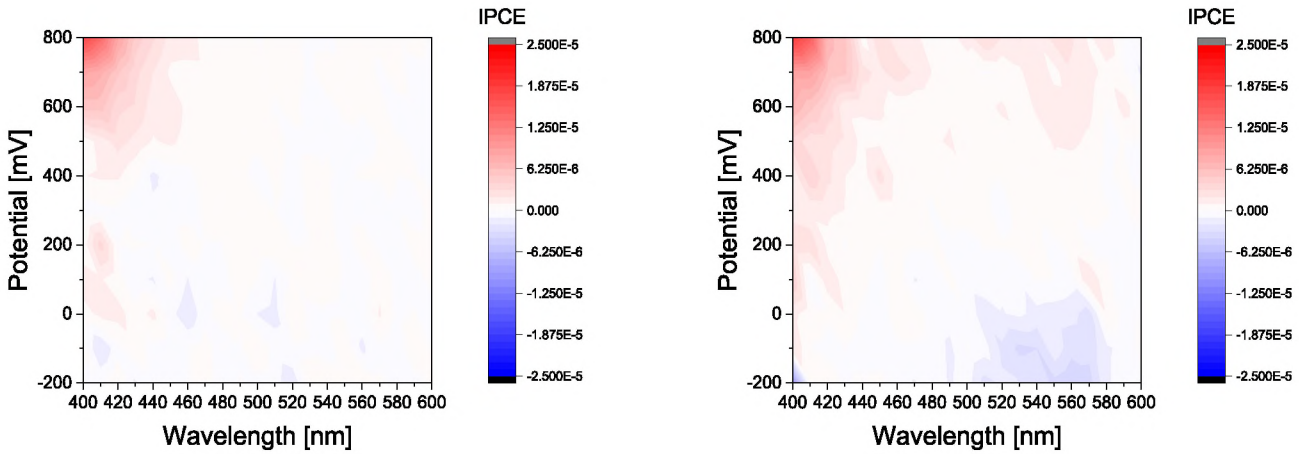

Fig. 6. IPCE measurements of TiO_2 (left) and TiO_2/RhB (right).

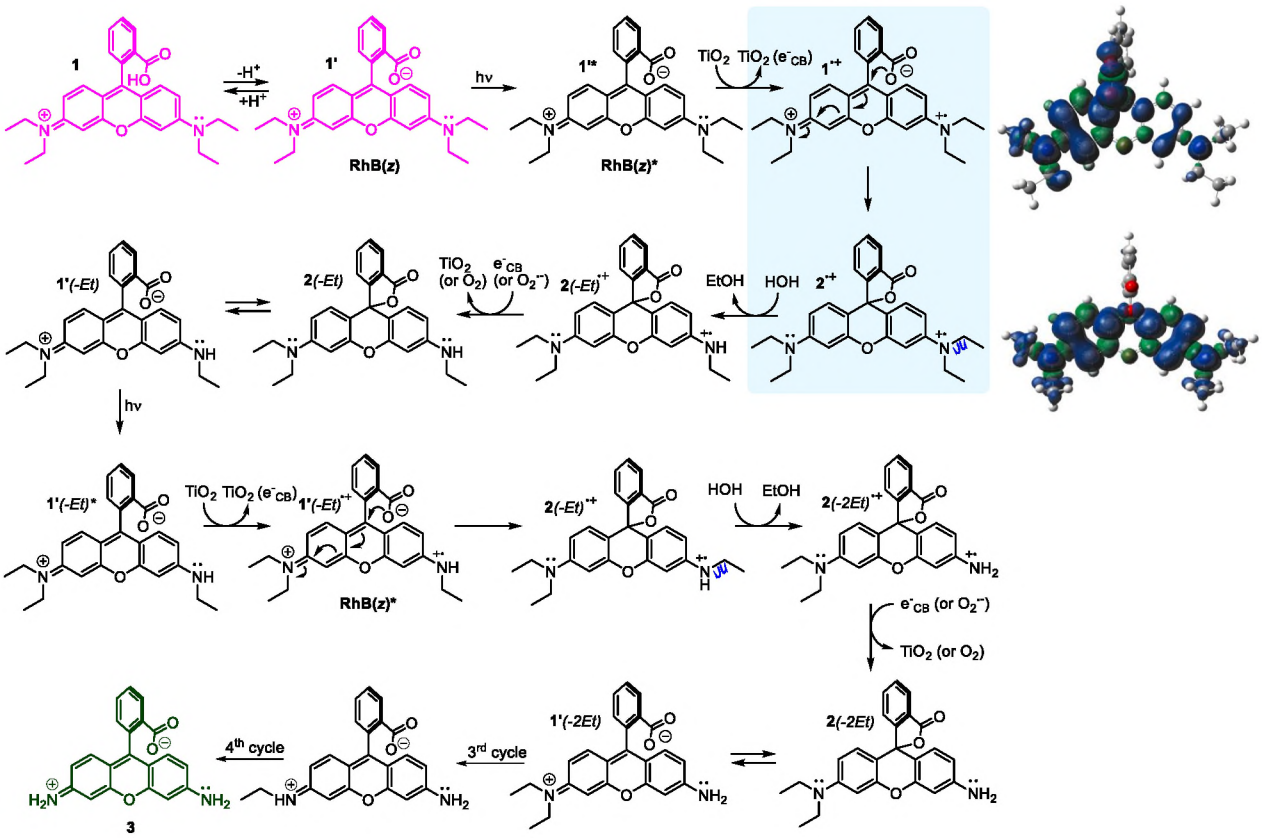

Scheme 2. The mechanism of the sequential *N*-deethylation of RhB.

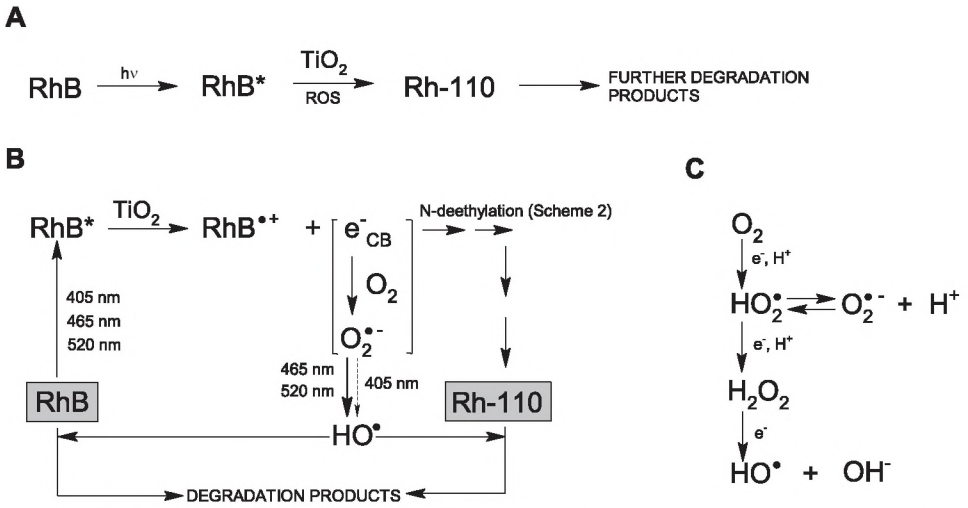

Scheme 3. RhB phototransformations in the presence of TiO_2: a) the most commonly referred mechanism encompassing selective *N*-deethylation involving HO•; b) the mechanism concluded from the present work encompassing two competitive reactions: *N*-deethylation and non-selective degradation involving HO• generated less efficiently upon 405 nm irradiation; c) consecutive steps of ROS generation resulting from O_2 reduction.

transfer between the adsorbed RhB molecule and the TiO_2 support (Scheme 3b). Electron transferred from the excited dye molecule to the conduction band of TiO_2 can be further utilized in the back electron transfer (compare Scheme 2) or in ROS formation (Scheme 3c). Irradiation at 465 or 520 nm results in efficient excitation of Rh-110 or RhB, respectively, thus generation of superoxide radicals should be also effective. In consequence, generation of hydroxyl radicals through the reductive pathway (Scheme 3c) leads to an extensive degradation of the dyes. However, excitation at 405 nm cannot lead to an efficient ROS generation, therefore, under such conditions the RhB to Rh-110 transformation prevails over the degradation processes.

Our studies shine a new light on the mechanism of phototransformation of RhB to Rh-110 indicating that the photochemistry of the adsorbed RhB should be taken into account when this dye is used in studies of the activity of photocatalytic systems.

CRediT authorship contribution statement

Anna Jakimińska: Conceptualization, Investigation, Formal Analysis, Data curation, Writing – original draft, Writing – review & editing,

Visualization. **Miłosz Pawlicki:** Writing – review & editing, Writing – original draft, Methodology, Formal analysis. **Wojciech Macyk:** Writing – review & editing, Writing – original draft, Supervision, Methodology, Funding acquisition, Formal analysis, Conceptualization.

Declaration of Competing Interest

The authors declare that they have no known competing financial interests or personal relationships that could have appeared to influence the work reported in this paper.

Data availability

Data will be made available on request.

Acknowledgements

This work was financially supported by the National Science Centre (Poland) – project OPUS 14 (2017/27/B/ST3/02457).

Appendix A. Supplementary data

Supplementary data to this article can be found online at https://doi.org/10.1016/j.jphotochem.2022.114176.

References

[1] T. Wu, G. Liu, J. Zhao, H. Hidaka, N. Serpone, Photoassisted Degradation of Dye Pollutants. V. Self-Photosensitized Oxidative Transformation of Rhodamine B under Visible Light Irradiation in Aqueous TiO_2 Dispersions, J Phys. Chem. B 102 (30) (1998) 5845–5851.

[2] L. Liu, S.Y. Lim, C.S. Law, B. Jin, A.D. Abell, G. Ni, A. Santos, Light-confining semiconductor nanoporous anodic alumina optical microcavities for photocatalysis, J Mater. Chem. A 7 (2019) 22514–22529, https://doi.org/10.1039/C9TA08585H.

[3] H. Liang, Z. Jia, H. Zhang, X. Wang, J. Wang, Photocatalysis oxidation activity regulation of Ag/TiO_2 composites evaluated by the selective oxidation of Rhodamine B, Appl. Surf. Sci. 422 (2017) 1–10, https://doi.org/10.1016/j.apsusc.2017.05.211.

[4] O. Merka, V. Yarovyi, D.W. Bahnemann, M. Wark, pH-Control of the Photocatalytic Degradation Mechanism of Rhodamine B over $Pb_3Nb_4O_{13}$, J Phys. Chem. C 115 (2011) 8014–8023, https://doi.org/10.1021/jp108637r.

[5] F. Chen, J. Zhao, H. Hidaka, Highly selective deethylation of rhodamine B: Adsorption and photooxidation pathways of the dye on the TiO_2/SiO_2 composite photocatalyst, Int. J Photoenergy 5 (2003) 209–217, https://doi.org/10.1155/S1110662X03000345.

[6] K. Spilarewicz-Stanek, A. Jakimińska, A. Kisielewska, D. Batory, I. Piwoński, Understanding the Role of Silver Nanostructures and Graphene Oxide Applied as Surface Modification of TiO_2 in Photocatalytic Transformations of Rhodamine B under UV and Vis Irradiation, Materials 13 (2020) 4653, https://doi.org/10.3390/ma13204653.

[7] W. Shi, W.X. Fang, J.C. Wang, X. Qiao, B. Wang, X. Guo, pH-controlled mechanism of photocatalytic RhB degradation over g-C_3N_4 under sunlight irradiation, Photochem. Photobiol. Sci. 20 (2021) 303–313, https://doi.org/10.1007/s43630-021-00019-9.

[8] Q. Yuan, C. Su, Y. Cao, K. Wu, J. Xu, S. Yang, Rhodamine loading and releasing behavior of hydrogen-bonded poly(vinylpyrrolidone)/poly(acrylic acid) film, Colloids Surf. A Physicochem. Eng. Asp. 456 (2014) 153–159, https://doi.org/10.1016/j.colsurfa.2014.05.030.

[9] H. Fu, S. Zhang, T. Xu, Y. Zhu, J. Chen, Photocatalytic Degradation of RhB by Fluorinated Bi_2WO_6 and Distributions of the Intermediate Products, Environ. Sci. Technol. 42 (2008) 2085–2091, https://doi.org/10.1021/es702495w.

[10] R. Lucena, J.C. Conesa, Photocatalysis with octahedral sulphides, in: X. Wang, M. Anpo, X. Fu (Eds.), Current Developments in Photocatalysis and Photocatalytic Materials – New Horizons in Photocatalysis, Elsevier, 2020, pp. 393–400, https://doi.org/10.1016/B978-0-12-819000-5.00024-2.

[11] X. Li, J. Ye, Photocatalytic Degradation of Rhodamine B over $Pb_3Nb_4O_{13}$/Fumed SiO_2 Composite under Visible Light Irradiation, J Phys. Chem. C 111 (2007) 13109–13116, https://doi.org/10.1021/jp072752m.

[12] P. Zhang, Z. Hu, Y. Wang, Y. Qin, X.W. Sun, W. Li, J. Wang, Enhanced photovoltaic properties of dye-sensitized solar cell based on ultrathin 2D TiO_2 nanostructures, Appl. Surf. Sci. 368 (2016) 403–408, https://doi.org/10.1016/j.apsusc.2016.02.010.

[13] A.M. Collins, X. Zhang, J.J. Scragg, G.J. Blanchard, F. Marken, Triple Phase Boundary Photovoltammetry: Resolving Rhodamine B Reactivity in 4-(3-Phenylpropyl)-Pyridine Microdroplets, ChemPhysChem 11 (2010) 2862–2870, https://doi.org/10.1002/cphc.200000094.

[14] K. Qi, F. Zasada, W. Piskorz, P. Indyka, J. Gryboś, M. Trochowski, M. Buchalska, M. Kobielusz, W. Macyk, Z. Sojka, Self-Sensitized Photocatalytic Degradation of Colorless Organic Pollutants Attached to Rutile Nanorods—Experimental and Theoretical DFT+D Studies, J Phys. Chem. C 120 (2016) 5442–5456, https://doi.org/10.1021/acs.jpcc.5b10983s.

[15] P. Łabuz, R. Sadowski, G. Stochel, W. Macyk, Visible light photoactive titanium dioxide aqueous colloids and coatings, Chem. Eng. J 230 (2013) 188–194, https://doi.org/10.1016/j.cej.2013.06.079.